

# Influence of heating atmosphere on the properties of stannous phosphate glass

Jiin-Jyh Shyu · Chih-Hsien Yeh

Received: 29 May 2010 / Accepted: 3 November 2010 / Published online: 23 November 2010  
© Springer Science+Business Media, LLC 2010

**Abstract** A low-viscosity 60 SnO–40 P<sub>2</sub>O<sub>5</sub> (mol%) glass was reheated at 280 °C (about 45 °C above the glass-transition temperature) for 20 min in various atmospheres (Ar, air, and O<sub>2</sub>), then the structure- and surface-related properties were examined. It was found that increase in P<sub>O<sub>2</sub></sub> increases surface hardness, reduces optical transmittance, and improves chemical durability. The above phenomena are explained in terms of the increased oxidation tendency of Sn<sup>2+</sup> to Sn<sup>4+</sup> on the glass surface during reheating in increased P<sub>O<sub>2</sub></sub>.

## Introduction

SnO–P<sub>2</sub>O<sub>5</sub> glasses generally present low glass-transition temperature and dilatometric softening temperature which make them suitable for low temperature sealing applications. Properties of SnO–P<sub>2</sub>O<sub>5</sub>-based glasses are studied for new optical materials [1], anode materials of lithium secondary batteries [2], and Pb-free sealing frits [3–6]. Nevertheless, the phosphate glasses present a poor chemical durability that limits their use. The addition of oxides, such as SnO, SiO<sub>2</sub>, Al<sub>2</sub>O<sub>3</sub>, PbO, PbF<sub>2</sub>, or B<sub>2</sub>O<sub>3</sub>, in the vitreous matrix can remarkably improve the chemical durability of phosphate glasses [7–10]. Nitridation, the substitution of nitrogen for oxygen in glass structure during melting process is able to improve the chemical durability of phosphate glasses [11–13]. Morena [14] reported that a decrease in durability when P<sub>2</sub>O<sub>5</sub> contents exceed 30–33 mol% immersed in 90 °C D.I. water of the SnO–ZnO–P<sub>2</sub>O<sub>5</sub> glasses. In our previous

study [15], the glasses with ≥40 mol% P<sub>2</sub>O<sub>5</sub> and higher Sn/(Sn + Mg) ratios showed reduced chemical durability. Several studies on SnO-containing glasses [16–21] indicate that a small amount of Sn<sup>4+</sup> coexists with Sn<sup>2+</sup> ions in the glass structure, even if the raw materials for tin contain only Sn<sup>2+</sup> ions. The Sn<sup>4+</sup>/Sn<sup>2+</sup> ratio depends on raw materials, glass composition, and melting conditions, etc. The contamination of tin near the surface of soda-lime-silica float glass has also been studied [22–25], showing that Sn<sup>2+</sup> and Sn<sup>4+</sup> coexist and that heat treatment at, e.g., 740 °C, causes the oxidation of Sn<sup>2+</sup> into Sn<sup>4+</sup> [23, 24]. According to our previous studies on SnO–MgO–P<sub>2</sub>O<sub>5</sub> glass [15, 26], to avoid serious oxidation of Sn<sup>2+</sup> to Sn<sup>4+</sup> during melting at 950–1200 °C addition of around 1 wt% of sugar and a nitrogen atmosphere are necessary. To the best knowledge of the authors, no studies focus on the effect of oxidation of Sn<sup>2+</sup> to Sn<sup>4+</sup> near the surface region of the glass during heating below 500 °C on properties of SnO–P<sub>2</sub>O<sub>5</sub>-based glasses. In our previous study [27], the water durability of the SnO–MgO–P<sub>2</sub>O<sub>5</sub> glass powder can be improved using Ar or air atmospheres for lower sintering temperatures (e.g., 380 and 410 °C) and using O<sub>2</sub> atmosphere for higher sintering temperatures (e.g., 470 °C).

In this article, effects of heating atmosphere (Ar, air, and O<sub>2</sub>) on the crystallization, surface state, and water durability of a 60 SnO–40 P<sub>2</sub>O<sub>5</sub> (mole%) cast glass were investigated.

## Experimental procedures

### Sample preparation

Glass with a nominal composition of 60 SnO–40 P<sub>2</sub>O<sub>5</sub> (mol%) was prepared from reagent-grade Sn<sub>2</sub>P<sub>2</sub>O<sub>7</sub> and

J.-J. Shyu (✉) · C.-H. Yeh  
Department of Materials Engineering, Tatung University,  
Taipei 104, Taiwan  
e-mail: jjshyu@ttu.edu.tw

$\text{NH}_4\text{H}_2\text{PO}_4$ . Well-mixed powder containing these chemicals and 1 wt% of sugar was placed in an alumina crucible. The batch was then placed in a furnace at 950 °C in a nitrogen atmosphere. The combination of nitrogen and sugar produced a reducing atmosphere during melting, inhibiting the oxidation of  $\text{Sn}^{2+}$  to  $\text{Sn}^{4+}$ . After heating for 15 min, the melt was quenched by pouring it onto a copper plate. The glass was then annealed at 260 °C for 3 h and furnace-cooled to room temperature.

The as-annealed glass was cut by diamond saw to yield square-shaped samples. The samples were polished and then ultrasonically cleaned with acetone, deionized water, and alcohol. The samples were then placed on soda-lime-silicate glass substrates, and were heated at a rate of 10 °C/min to 280 °C and held for 20 min, then furnace cooled. Atmospheres of Ar, air, and  $\text{O}_2$  were applied during the heating process.

### Characterization

The crystallization temperature of the glass during heating from room temperature to 500 °C was measured by differential thermal analysis (DTA, model SDT 2960, TA Instruments, New Castle, DE, USA) at a heating rate of 10 K/min. Flowing Ar, air, and  $\text{O}_2$  (100 mL/min) were applied during the thermal analysis. Phase identification of the heated samples was conducted by X-ray diffraction (XRD) analysis. Measurements were performed on a diffractometer (model X'Pert PRO, PANalytical B.V., Almelo, Netherlands) with  $\text{Cu K}\alpha$  radiation. The operating power was 40 kV and 45 mA. A sampling time of 1 s for each interval of  $0.02^\circ$  ( $2\theta$ ) was used. Raman spectra of the samples were measured using micro-Raman spectrometry (model inVia, Renishaw, Gloucestershire, UK) between 400 and  $1400\text{ cm}^{-1}$  with a resolution of  $1\text{ cm}^{-1}$ . A 325 nm line of He–Cd laser was used as the excitation light. The transmittance curves (200–900 nm) of the samples were measured by spectrophotometry (model V560, Jasco International Co. Ltd., Tokyo, Japan). The sample thickness was 1.0 mm. Vickers microhardness of the samples was measured using a microhardness tester (model Fischerscope HM 2000M, Fischer, Germany) with a 100 mN load for 20 s and indentation depth for 0.2  $\mu\text{m}$ . Six random measurements were done on each sample. The samples were coated with a thin film of gold for scanning electron microscopy (SEM, model JSM-5600, Jeol, Tokyo, Japan) observations. In the water durability test, the samples were placed in covered polypropylene flasks containing 100 ml of deionized water at 40 °C for 120 min. The reactor was agitated with a shaking rate of 100 rpm. At least three samples were used for each heating condition. Finally, weight loss per unit surface area was calculated.

## Results and discussion

### Thermal analysis of the glass

Chemical analysis of as-annealed glass shows that the glass composition consists of 56.90 SnO, 41.14  $\text{P}_2\text{O}_5$ , and 1.96  $\text{Al}_2\text{O}_3$  (mol%) which comes from the alumina crucible. Figure 1 shows the DTA thermograms of the as-annealed glass heated in various atmospheres. The glass-transition temperature ( $T_g$ ) is about 244 °C and is almost unchanged with the change in  $\text{P}_{\text{O}_2}$ . No obvious exothermic peaks appeared before 500 °C except in Ar atmosphere. To explore this point, as-annealed glass heated at 475 °C for 20 min in various atmospheres were examined. With air and  $\text{O}_2$  atmospheres, the 475 °C-heated glasses are amorphous according to XRD and microstructural analyses (the data are not shown in this article). However, the as-heated surface of the glass heated in Ar atmosphere reveals crystalline signals (Figs. 2, 3). The crystalline phase cannot be identified because the diffraction lines are too less (Fig. 2). According to EDS analysis, the crystalline phase (indicated by the arrows in Fig. 3) is Sn-bearing phosphate. After removing the free surface by polishing the sample, the crystalline signals vanish (Fig. 2). According to the above results, it is suggested that the increase in  $\text{P}_{\text{O}_2}$  at 475 °C might increase the oxidation tendency of  $\text{Sn}^{2+}$  to  $\text{Sn}^{4+}$  on the sample surface. Williams et al. [23] have investigated the oxidation of  $\text{Sn}^{2+}$  to  $\text{Sn}^{4+}$  on the tin side of soda-lime-silica float glass and show that  $\text{Sn}^{2+}$  is less tightly bound than  $\text{Sn}^{4+}$ . The single-bond strength values for  $\text{Sn}^{2+}\text{-O}$  and  $\text{Sn}^{4+}\text{-O}$  are 46 [28] and 133 kcal/mol [29], respectively. Moreover, Takeda et al. [30] have shown that the oxidation of  $\text{Sn}^{2+}$  to  $\text{Sn}^{4+}$  by oxygen diffusion may subsequently cause the change in the coordination structure of tin from tetragonally pyramidal ( $\text{Sn}^{2+}$ ) to octahedral ( $\text{Sn}^{4+}$ ) in tin-soda-lime silica glass.

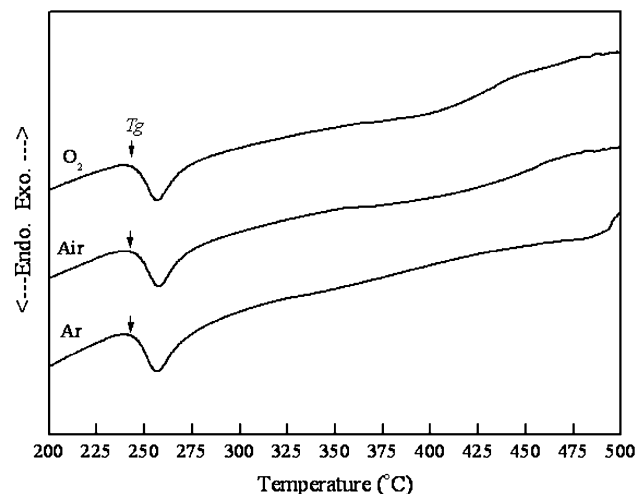


**Fig. 1** DTA thermograms of the as-annealed glass heated in various atmospheres

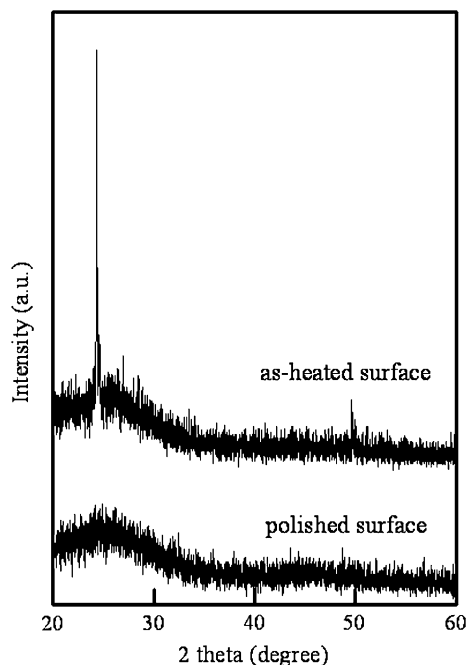


**Fig. 2** XRD patterns of the glass heated at 475 °C for 20 min in Ar

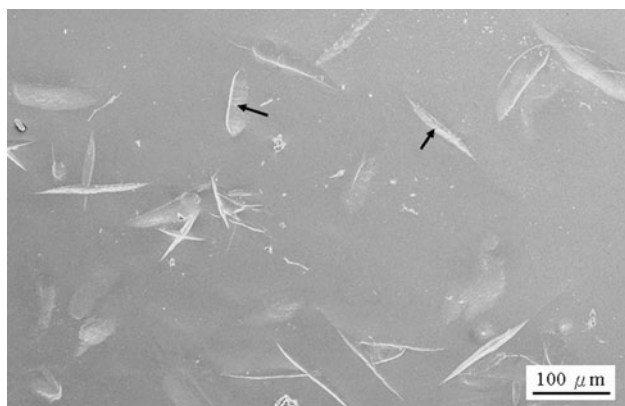


**Fig. 3** Micrographs of the as-heated surface of the glass heated at 475 °C for 20 min in Ar

Meanwhile, the bonding changes from covalent ( $\text{Sn}^{2+}\text{-O}$ ) to ionic ( $\text{Sn}^{4+}\text{-O}$ ) in nature. Bhat et al. [20] have suggested that the SnO in the  $\text{SnO-NaPO}_3$  glass acts as a modifier up to about 27 mol% of nominal composition. Above this concentration, SnO acts as a glass former.  $\text{SnO}_2$ , however, is always found to behave as a glass former. In this study, the stronger  $\text{Sn}^{4+}\text{-O}$  bond than the  $\text{Sn}^{2+}\text{-O}$  bond would increase the viscosity of the glass on the sample surface, thus reducing the crystallization tendency of the surface region.

Because of the low glass-transition temperature ( $T_g = 244$  °C) of the present  $\text{SnO-P}_2\text{O}_5$  glass, it is wonder whether oxidation of  $\text{Sn}^{2+}$  to  $\text{Sn}^{4+}$  occurs at lower temperatures. Therefore, in the following experiments, the glass reheated at 280 °C (i.e., about 45 °C above  $T_g$ ) for 20 min in various atmospheres were investigated.

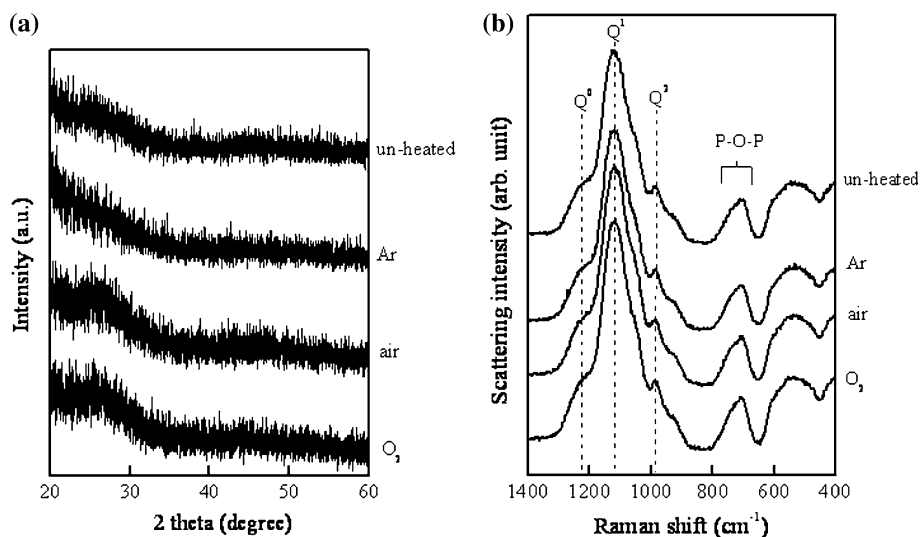
## Structural analyses

Figure 4a and b shows the XRD patterns and Raman spectra, respectively, of the unheated (as-annealed) glass and the glasses heated at 280 °C for 20 min in various atmospheres. Figure 5a–c shows the microstructures of the as-heated surfaces of the corresponding samples. All samples are amorphous in nature (Figs. 4a, 5a–c), consistent with that shown in DTA thermograms (Fig. 1). According to Fig. 4b, there are three bands in the range of  $900\text{--}1200\text{ cm}^{-1}$ , resulted from the symmetric stretching mode of  $(\text{PO}_2)^-$  ( $1240\text{ cm}^{-1}$ ,  $Q^2$  tetrahedral unit)  $(\text{PO}_3)^{2-}$  ( $1115\text{ cm}^{-1}$ ,  $Q^1$  tetrahedral unit), and  $(\text{PO}_4)^{3-}$  ( $970\text{ cm}^{-1}$ ,  $Q^0$  tetrahedral unit) [10, 31–33]. The bands at  $650\text{--}750\text{ cm}^{-1}$  are due to P–O–P stretching modes. Both the intensities of  $Q^2$ ,  $Q^1$ ,  $Q^0$  and P–O–P show no obvious difference with the change in  $P_{O_2}$ . The above structural analyses (XRD, microstructure, and Raman spectra) do not reveal the possible differences between the surfaces heated in various atmospheres at 280 °C, possibly because the oxidation layer is too thin to be detected.

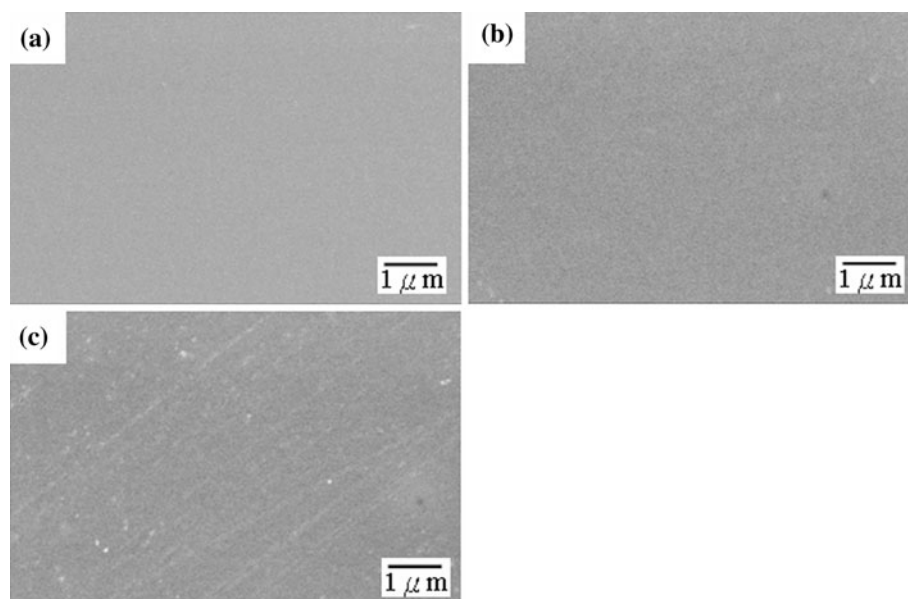
## Properties

Figures 6 and 7 show the Vickers microhardness and the variation of weight loss per unit area with immersion time in 40 °C water, respectively. Both data were taken from the polished surface of the unheated (as-annealed) glass and the as-heated surfaces of the glasses heated at 280 °C for 20 min in various atmospheres. The average dissolution rate (DR) for immersion time of 120 min, defined as the weight loss per unit surface area per unit time, was calculated. In comparison with the unheated glass, heating the glass in Ar slightly decreases hardness from 235 to 232  $\text{kg/mm}^2$  and increases DR from 3.55 to 4.52  $\mu\text{g/cm}^2\text{ min}$ . On the other hand, heating the glass in increased  $P_{O_2}$  is able to increase hardness from 232 (for Ar) to 250  $\text{kg/mm}^2$  (for  $O_2$ ) and reduce DR from 4.52 (for Ar) to 2.68  $\mu\text{g/cm}^2\text{ min}$  (for  $O_2$ ). It is noted that the variations of hardness and water durability (represented by  $\text{DR}^{-1}$ ) with heating atmosphere have the same trend, i.e., heating in Ar weakens the bondings while heating in increased  $P_{O_2}$  strengthens the bondings of the glass surface. At first, it is proposed that increase in bond strength after heating in oxidizing atmospheres might be caused by surface crystallization and/or increased oxidation-tendency of  $\text{Sn}^{2+}$  to  $\text{Sn}^{4+}$  on glass surfaces. It has been shown in Figs. 4a and 5 that the surfaces of all samples heated at 280 °C are amorphous in nature. Even if at 280 °C a crystalline film has formed on the glass surface (with a thickness which is too thin to be detected by XRD, SEM, and Raman analyses), increase in  $P_{O_2}$  will reduce crystallization tendency (according to the results on 475 °C as shown in Figs. 2, 3), thus reducing both hardness and water durability.

**Fig. 4** **a** XRD patterns and **b** Raman spectra of the unheated (as-annealed) glass and the glasses heated at 280 °C for 20 min in various atmospheres. For the heated glasses, the as-heated surfaces were examined



**Fig. 5** Micrographs of the as-heated surface of the glasses heated at 280 °C for 20 min in **a** Ar, **b** air, and **c** O<sub>2</sub>



It is thus suggested that the increase in both hardness and water durability with the increased P<sub>O<sub>2</sub></sub> shown in Figs. 6 and 7, respectively, is caused by oxidation of Sn<sup>2+</sup> to Sn<sup>4+</sup> on the glass surface. The stronger Sn<sup>4+</sup>–O bond than the Sn<sup>2+</sup>–O bond [23] would strengthen the glass structure within glass surface region. It has been found for tin-doped soda-lime-silica glass that Sn<sup>4+</sup> increases the glass modulus and that Sn<sup>2+</sup> possibly has a slight effect on the glass modulus [30, 34].

Other evidence supporting the formation of a surface oxidized layer after heating under air or oxygen atmospheres at 280 °C is given by the optical transmission data in the UV–visible range, as shown in Fig. 8. The heated glasses have reduced transmittances than that of the as-annealed glass, and the increase in P<sub>O<sub>2</sub></sub> lowered the transmittance of the heated glasses. Similar with that

described above, if a crystalline film has formed on the glass surface after reheating at 280 °C, increase in P<sub>O<sub>2</sub></sub> will decrease the crystallization tendency, thus increasing (instead of reducing) transmittance. It is suggested that the surface oxidized layer, due to its heterogeneous nature, would reduce transmittance of the glass. For soda-lime-silica float glass, it is generally accepted that the phenomenon of bloom after reheating the glass in air is related to the oxidation of Sn<sup>2+</sup> to Sn<sup>4+</sup> [35–38]. The differences in properties (e.g., viscosity, glass-transition temperature, Young’s modulus, and thermal-expansion coefficient) between the tin-rich layer and the glass result in the formation of wrinkling structure near the surface region [30, 34].

Glasses heated with a prolonged period of time (80 min) at 280 °C were also analyzed. They are still amorphous in

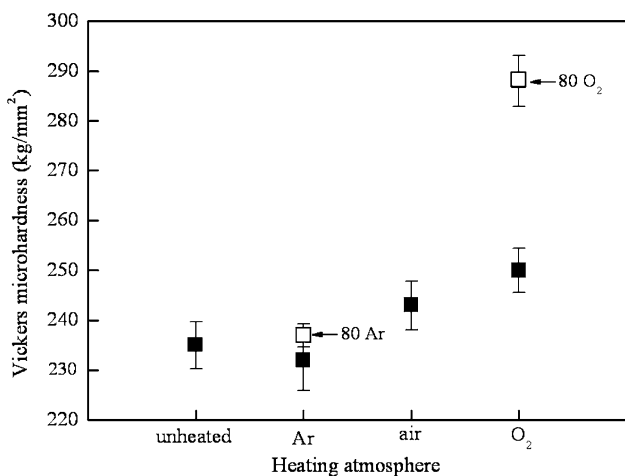


**Fig. 6** Vickers microhardness of the unheated glass and the glasses heated at 280 °C for 20 min in various atmospheres. For the heated glasses, the data were taken from the as-heated surfaces. *Open symbols* are glasses heated at 280 °C for 80 min in various atmospheres (80 Ar and 80 O<sub>2</sub> denoted the samples heated for a prolonged time at 280 °C in Ar and oxygen, respectively)

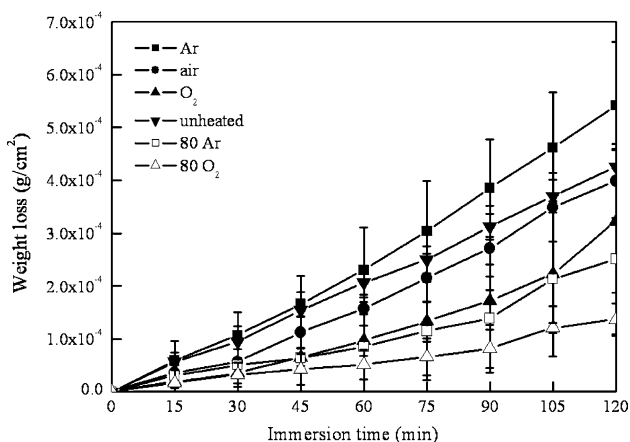


**Fig. 7** Variation of the weight loss per unit surface area in 40 °C water with immersion time of the unheated glass and the glasses heated at 280 °C for 120 min in various atmospheres. For the heated glasses, the as-heated surfaces were examined (80 Ar and 80 O<sub>2</sub> denoted the samples heated for a prolonged time at 280 °C in Ar and oxygen, respectively)

nature according to XRD and microstructural analyses (the data are not shown in this article). The appearances of heated glasses are still transparent. As shown in Figs. 6 and 7, in comparison with the unheated glass, heating the glass at 280 °C for 20 and 80 min in Ar slightly changed hardness from 235 to 232 and 237 kg/mm<sup>2</sup>, respectively, and the DR value first increased from 3.55 to 4.52, then decreased to 2.51 μg/cm<sup>2</sup> min. On the other hand, the prolonged heating time in O<sub>2</sub> is able to remarkably increase hardness (235 → 250 → 288 kg/mm<sup>2</sup>) and reduce DR (3.55 → 2.68 → 1.37 μg/cm<sup>2</sup> min). It is noted that the change of properties of the glass as a result of reheating at 280 °C is

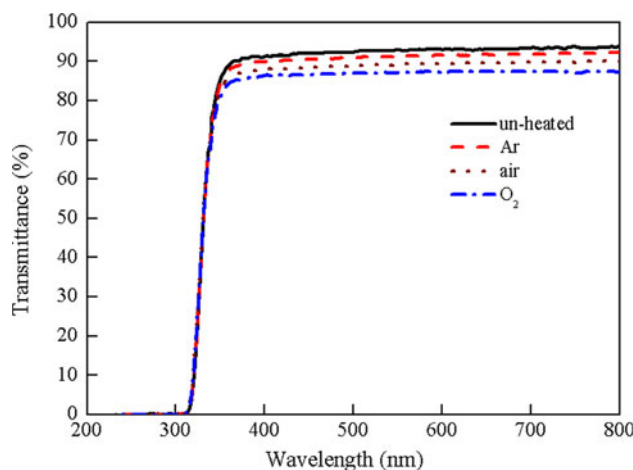


**Fig. 8** Transmission spectra in the UV–visible range of the unheated glass and the glasses heated at 280 °C for 20 min in various atmospheres (thickness 1.0 mm). For the heated glasses, the as-heated surfaces were examined

more sensitive to oxygen than Ar atmosphere. As shown in “[Thermal analysis of the glass](#),” heating in Ar atmosphere has a higher tendency to crystallization than in oxygen atmosphere. It is concluded that the strengthening of glass after heating in oxygen atmosphere should be caused by oxidation of Sn<sup>2+</sup> to Sn<sup>4+</sup>. The change of properties as a result of heating in Ar atmosphere is not clearly understood. It proposed that slight modification of glass surface structure (e.g., the penetration of a small amount of Ar and/or the formation of a crystalline film with a thickness which is too thin to be detected by XRD and SEM analyses) might be the cause.

In this study, it is suggested that the formation of oxidized (Sn<sup>4+</sup>-rich) layer after reheating the SnO–P<sub>2</sub>O<sub>5</sub> glass at 280 °C in air or O<sub>2</sub> results in increased hardness, decreased optical transmittance, and improved chemical durability. Moreover, because of the low *T<sub>g</sub>* (244 °C) of the present glass, the oxidation can occur at such a low temperature (280 °C), influencing the surface-related properties. For soda-lime-silica float glass, the surface oxidation of Sn<sup>2+</sup> to Sn<sup>4+</sup> is more apparent when the glass is reheated at higher temperatures (e.g., 500–730 °C [23, 35]) particularly above *T<sub>g</sub>* (generally <600 °C). Muñoz et al. [39] have studied the oxidation behavior of nitrated Li<sub>2</sub>O–Na<sub>2</sub>O–PbO–P<sub>2</sub>O<sub>5</sub> glass powders and show that the faster the decrease in viscosity during heating, the earlier and intense the oxidation.

**Conclusions**

A low-viscosity stannous phosphate (60 mol% SnO–40 mol% P<sub>2</sub>O<sub>5</sub>) glass was reheated at 280 °C (about 45 °C above *T<sub>g</sub>*) for 20 min under various atmospheres (Ar, air, and O<sub>2</sub>). It was found that the heating atmosphere



determines the surface-related properties. The increase in  $P_{O_2}$  increases surface hardness (up to 7% higher than the as-annealed glass), reduces optical transmittance (up to 6% lower than the as-annealed glass), and improves chemical durability (dissolution rate in 40 °C water can be reduced down to 33% lower than the as-annealed glass). Extending heating time to 80 min in  $O_2$  further increases surface hardness (up to 22.5% higher than the as-annealed glass) and improves chemical durability (up to two times higher than the as-annealed glass). The above phenomena are explained in terms of the increased oxidation tendency of  $Sn^{2+}$  to  $Sn^{4+}$  on the glass surface during reheating at 280 °C.

## References

1. Takebe H, Nonaka W, Kubo T, Cha J, Kuwabara M (2007) *J Phys Chem Solids* 68:983
2. Hayashi A, Konishi T, Tadanaga K, Minami T, Tatsumisago M (2004) *J Non-Cryst Solids* 345&346:478
3. Brow RK (2000) *J Non-Cryst Solids* 263&264:1
4. Brow RK, Tallant DR (1997) *J Non-Cryst Solids* 222:396
5. Morena R (1996) USP 5,514,629
6. Taketami K (2003) JP Patent 2003/252648
7. Shaw CM, Shelby JE (1988) *Phys Chem Glasses* 29:49
8. Donald IW (1993) *J Mater Sci* 28:2841. doi:[10.1007/BF00354689](https://doi.org/10.1007/BF00354689)
9. Shih PY, Yung SW, Chen CY, Liu HS, Chin TS (1997) *Mater Chem Phys* 50:63
10. Cha J, Kubo T, Takebe H, Kuwabara M (2008) *J Ceram Soc Jpn* 116:915
11. Pascual L, Durán A (1996) *Mater Res Bull* 31:77
12. Sauze AL, Marchand R (2000) *J Non-Cryst Solids* 263&264:285
13. Yung H, Shih PY (1997) *J Am Ceram Soc* 80:2213
14. Morena R (2000) *J Non-Cryst Solids* 263&264:382
15. Shyu JJ, Yeh CH (2007) *J Mater Sci* 42:4772. doi:[10.1007/s10853-006-0766-4](https://doi.org/10.1007/s10853-006-0766-4)
16. Sears A, Hölland D, Dowsett MG (2000) *Phys Chem Glasses* 41:42
17. Bekaert É, Montagne L, Delevoye L, Palavit G, Revel B (2004) *C R Chim* 7:377
18. Hölland D, Smith ME, Poplett IJF, Johnson JA, Thomas MF, Bland J (2001) *J Non-Cryst Solids* 293–295:175
19. Nishida T, Katada M, Osawa N, Sato R, Komatsu T, Matusita K (1994) *Hyperfine Interact* 94:2119
20. Bhat MH, Berry FJ, Jiang JZ, Rao KJ (2001) *J Non-Cryst Solids* 291:93
21. Bekaert E, Montagne L, Delevoye L, Palavit G, Wattiaux A (2004) *J Non-Cryst Solids* 345&346:70
22. Williams KFE, Johnson CE, Nikolov O, Thomas MF (1998) *J Non-Cryst Solids* 242:183
23. Williams KFE, Johnson CE, Greengrass J, Tilley BP, Gelder D, Johnson JA (1997) *J Non-Cryst Solids* 211:164
24. Takeda S, Akiyama R, Hosono H (2001) *J Non-Cryst Solids* 281:1
25. Principi G, Maddalena A, Gupta A, Geotti-Bianchini F, Hreglich S, Verità M (1993) *Nucl Instrum Methods Phys Res B* 76:215
26. Shyu JJ, Yeh CH (2009) *J Mater Sci* 44:2985. doi:[10.1007/s10853-009-3396-9](https://doi.org/10.1007/s10853-009-3396-9)
27. Shyu JJ, Yeh CH (2010) *J Mater Sci* (accepted). doi:[10.1007/s10853-010-4861-1](https://doi.org/10.1007/s10853-010-4861-1)
28. Kingery WD, Bowen HK, Uhlmann DR (1976) *Introduction to ceramics*, 2nd edn. Wiley, New York, p 99
29. Max NY (1993) USP 5,225,366
30. Takeda S, Akiyama R, Hosono H (2002) *J Non-Cryst Solids* 311:273
31. Cha J, Kawano M, Takebe H, Kuwabara M (2008) *J Ceram Soc Jpn* 116:1100
32. Schwarz J, Tichá H, Tichý L, Mertens R (2004) *J Optoelectron Adv Mater* 6:737
33. Takebe H, Baba Y, Kuwabara M (2006) *J Non-Cryst Solids* 352:3088
34. Krohn MH, Hellmann JR, Mahieu B, Pantano CG (2005) *J Non-Cryst Solids* 351:455
35. Howell JA, Hellmann JR, Muhlstein CL (2008) *J Non-Cryst Solids* 354:1891
36. Frischat GH (2002) *C R Chim* 5:759
37. Pilkington LAB (1969) *Proc R Soc Lond A* 314:1
38. Williams KFE, Thomas MF, Greengrass J, Bradshaw JM (1999) *Glass Technol* 40:103
39. Muñoz F, Pascual L, Durán A, Rocherullé J, Marchand R (2006) *J Eur Ceram Soc* 26:1455